

Nanocarriers made from non-ionic surfactants or natural polymers for pulmonary drug delivery.

Carter K.C. and M. Puig-Sellart, Strathclyde Institute of Pharmacy and Biomedical Sciences, University of Strathclyde, 161 Cathedral Street, Glasgow, G4 0RE, UK

**Corresponding author**

Dr K. C. Carter, Strathclyde Institute of Pharmacy and Biomedical Sciences, University of Strathclyde, 161 Cathedral Street, Glasgow, G4 0RE, UK.

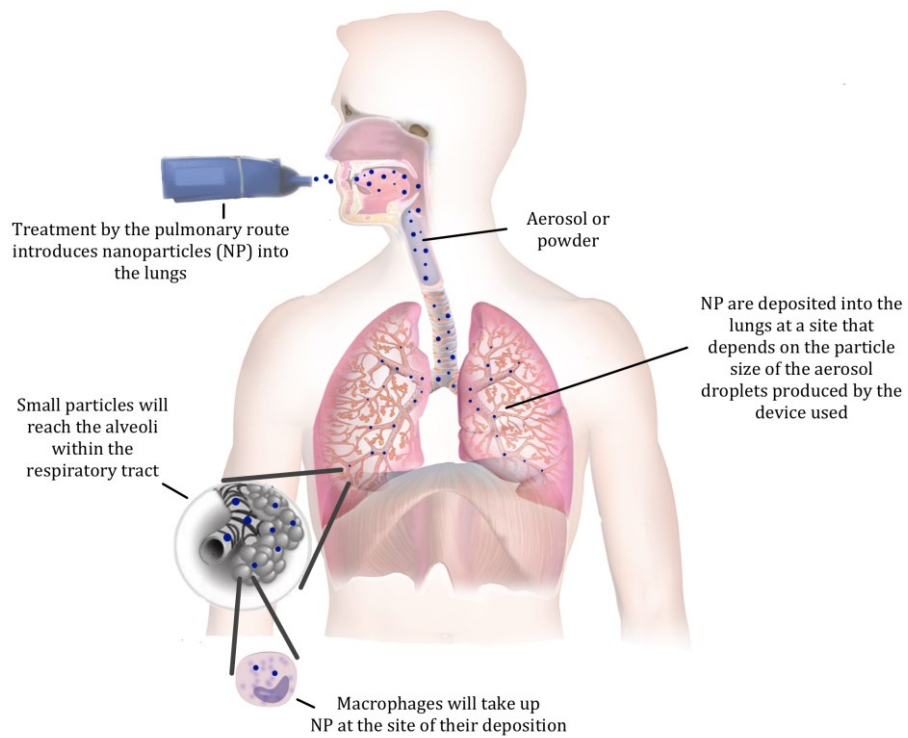
Email: k.carter@strath.ac.uk

Tel: 0141 548 3823

Fax 0141 552 2562

**Keywords:** drug delivery systems, non-ionic surfactant vesicles, nanoparticles, pulmonary

## Graphical abstract



1 **Abstract**

2 Treatment by the pulmonary route can be used for administration of drugs that act  
3 locally in the lungs (e.g. treatment of lung cancer, chronic obstructive pulmonary  
4 disease, asthma) or non-invasive administration of drugs that act systemically. The  
5 potential of drug delivery systems formed from non-ionic surfactants or natural  
6 products i.e. proteins and polysaccharides for pulmonary delivery are discussed.

7

8 **Introduction**

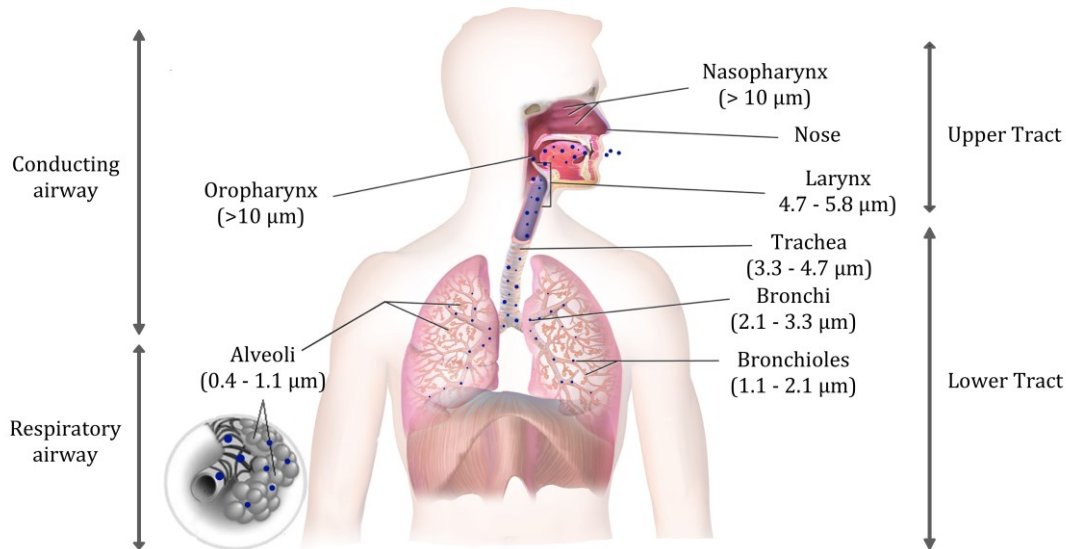
9

10 Treatment by inhalation can be used to deliver drugs directly to the lungs to treat  
11 conditions such as lung cancer, tuberculosis, cystic fibrosis or asthma; or as a means  
12 of treating systemic conditions such as diabetes or analgesia and the pulmonary drug  
13 delivery market is estimated to be worth £28.7million by 2019 [1]. Treatment by  
14 inhalation is more patient friendly than parenteral injection. It also allows the drug to  
15 avoid the first pass metabolism which occurs in the liver, and the concentration of  
16 metabolising enzymes such as CYP450 is lower in the lungs compared to other organs  
17 [2]. However successful drug delivery via this route requires production of a drug  
18 formulation that is effective, stable and safe but it must also be suitable for inhalation  
19 and have the correct characteristics to reach the appropriate site within the lungs.  
20 Additionally a drug must evade the innate defense mechanisms present in the lungs,  
21 such as mucociliary clearance and macrophage uptake before it reaches its site of  
22 action [3]. The lungs are primarily designed for gas exchange and have a symmetric  
23 dichotomously branching structure (Figure 1). The upper respiratory tract consists of  
24 the nasal cavity and pharynx and the lower respiratory tract consists of the larynx,  
25 trachea, bronchi, bronchioles and alveoli [4]. The surface area of the lungs increases  
26 from 2 m<sup>2</sup> in the upper respiratory tract to 103 m<sup>2</sup> in the lower airways. And cell  
27 thickness decreases from 60 µm in the bronchi to 0.1 µm in the alveoli. Aerosol particle  
28 size is a key parameter in defining the drug deposition within the lungs. Aerosols with  
29 a small particle size (< 2 µm) are distributed in the peripheral airways, whereas larger  
30 aerosols (> 5 µm) are deposited in the central area of the lungs. Particles are deposited  
31 in the lungs by inertial impaction, gravitational sedimentation or Brownian diffusion.  
32 Inertial impaction predominates, as large particles (> 10 µm) cannot follow the fast

33 airflow in the conducting airways, and impact into the walls of the upper  
34 tracheobronchial region. Particles that impact on the mucus barrier are then cleared  
35 by the mucociliary escalator system, where ciliated epithelium moves mucus  
36 entrapped particles towards the pharynx where they are removed by macrophages or  
37 expectorated [5]. Smaller aerosol particles ( $< 5 \mu\text{m}$ ) sediment in the bronchi and  
38 bronchioles or reach the alveoli, where they are exposed to Brownian diffusion as the  
39 air velocity is negligible within the alveoli. Thus aerosol particles between 1 and  $5 \mu\text{m}$   
40 can reach the lower respiratory system [6]. Very small particles ( $< 0.1 \mu\text{m}$ ) cannot be  
41 deposited in the airways as they are breathed out easily [7]. The optimal site of aerosol  
42 deposition depends on the particular application. For instance, the  $\beta_2$  agonist  
43 salbutamol should be delivered to the peripheral areas of the lungs as  $\beta_2$  receptors are  
44 located in the bronchi and bronchioles [8] whereas the muscarinic antagonist  
45 ipratropium bromide, should be deposited in the conducting airways as muscarinic  
46 M3 receptors are predominant in the conducting airways [9]. For the treatment of  
47 systemic diseases, the inhaled drug should be deposited in the peripheral areas that  
48 are rich in alveoli, where systemic absorption is facilitated by the thin alveolar-vascular  
49 barrier [10]. Drug deposition can also be influenced by pathological  
50 bronchoconstriction, inflammation or airway obstruction, leading to uneven or central  
51 deposition of the drug formulation within the respiratory tract [11, 12].

52

53



54

55 **Figure 1** Areas of the respiratory system based on physiological characteristics or  
 56 anatomical parts. Inhaled aerosols are deposited in different areas of the respiratory  
 57 system according to their droplet size (adapted [10,13,14]).  
 58

59

### 60 **Influence of the inhalation device**

61 The development of an effective inhaled therapy depends on the pharmacology of the  
 62 active ingredients, its aerosolisation characteristics and the efficiency of the aerosol  
 63 generating device e.g. pressurised metered-dose inhaler, dry powder inhaler or  
 64 nebuliser. There are a wide range of pulmonary devices [15] and new generation  
 65 inhalers are very efficient at producing aerosols with well characterised properties.  
 66 Thus has lead to more effective targeting of the nebulised drug formulation to the  
 67 lungs, which can lead to the development of a specialised drug-device combination  
 68 for a particular application. Some inhalers have added adaptations to increase 'ease of  
 69 use', which is of particular importance for therapies directed towards patients with an  
 70 older patient profile, or the ability to obtain data on the dose delivered to the patient  
 71 [16].  
 72

73 It is possible to measure the aerosol particle size *in vitro* using an impactor, where an  
 74 aerosol hits a flat surface and is separates into different size ranges depending on  
 75 where it lands in the impactor or impingers. The newest impactor described in the  
 76 European Pharmacopoeia is the next generation impactor (NGI), which is the only

77 impactor that works horizontally and collects the aerosol droplets on cups of different  
78 cut-off diameter. It has seven stages and a micro orifice collector. The European  
79 Pharmacopoeia describes one twin and three multistage apparatus [17]. The twin  
80 impinger is operated at a flow rate of 60 L/min and has a cut-off diameter of 6.4  $\mu\text{m}$ .  
81 This meaning that particles found in the second stage correspond to the respirable  
82 portion ( $< 6.4 \mu\text{m}$ ). The multi-stage liquid impinger (MSLI), can be used at different air  
83 flows, and has a mouth piece attached to the aerosol device, 4 stages and filter paper  
84 in the fifth compartment collects the remaining particles. The advantage of the MSLI  
85 over other impactors is the presence of solvent in each collection stage. This is  
86 important, as it avoids the re-entrainment phenomena of aerosol droplets being  
87 reincorporated into the airflow, particularly with DPIs. The data obtained using any of  
88 the multi-stage impingers or impactors can be used to calculate the aerodynamic  
89 aerosol size distribution of an aerosolised formulation. The mass median aerodynamic  
90 diameter (MMAD) of an active ingredient is the diameter at which 50 % of the particles  
91 by mass are bigger than the other 50 %. The MMAD is calculated when the log-normal  
92 distribution of the mass-weighted data is assumed by plotting a base ten logarithm  
93 cut-off diameter against cumulative percentage undersize [18]. The distribution of the  
94 particles in the apparatus is generally described by the geometric standard deviation  
95 (GSD) and a GSD closer to the one indicates a mono-distributed aerosol size. Fine  
96 particle fraction (FPF  $< 5 \mu\text{m}$ ) is the fraction of the aerosol mass contained in particles  
97 with an aerodynamic diameter smaller than 5  $\mu\text{m}$  and larger than 0.98  $\mu\text{m}$ . Achieving  
98 a low MMAD and a GSD close to the one indicates a fine aerosol size with a tight size  
99 distribution. However, the aerodynamic aerosol size distribution calculated with  
100 impactor techniques can only be classified into a small number of size ranges  
101 depending on the number of stages of the apparatus. For example, the twin impactor  
102 possesses one cut-off diameter and the NGI seven. Electrostatic charge and fine  
103 particle adhesion on the walls of the apparatus and losses between stages may also  
104 disturb particle collection. Another way to characterize aerosol characteristics is to  
105 use laser diffraction techniques. These are easy-to-use and can analyse particles over  
106 a broad size range. In addition, the measurement is fast, non-flow dependent and  
107 possess automatic data recording. A unique characteristic of laser diffraction methods  
108 is being able to carry out time measurements of the cloud distribution [19] and analyse

109 multi-modal drop size aerosol distribution [20]. However, low particle concentration  
110 may lead to low laser obstruction so the aerosol cloud may not be able to be  
111 measured. Laser diffraction does not measure aerodynamic diameter. Instead, it  
112 measures geometric diameter in terms of mass median diameter (MMD). This value  
113 does not consider particle density and assumes that particles are spherical. Pilcer *et*  
114 *al.* [21] compared the values of respiratory fraction obtained with MSLI and the NGI  
115 with the values acquired from laser diffraction techniques when powder formulations  
116 were aerosolised. The data obtained from the impactor and the laser diffraction  
117 differed. However, they found a good correlation factor between both aerodynamic  
118 diameter and geometric diameter results.

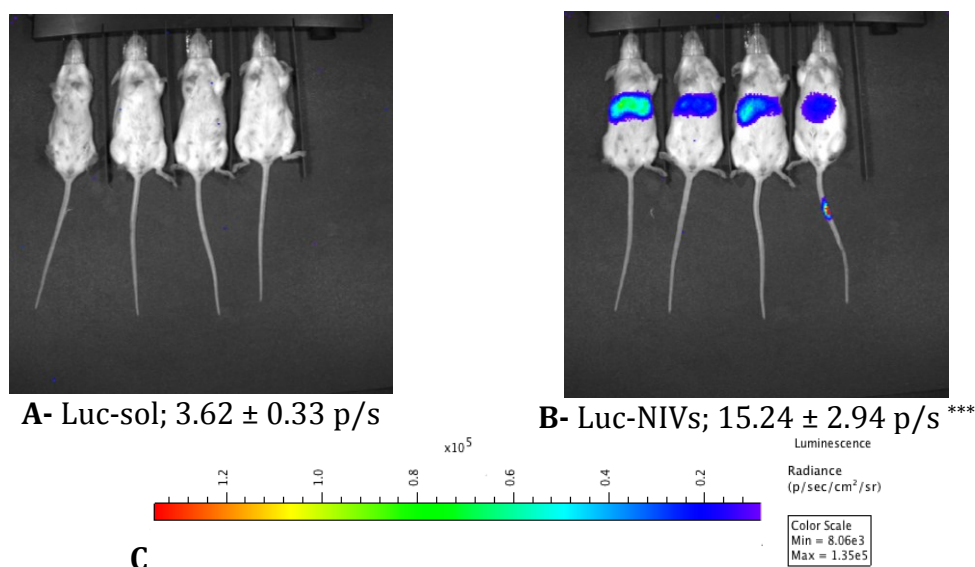
119

## 120 **Animal studies**

121 Animal models have been extensively used to investigate the effect of inhaled drug  
122 therapies [22, 23]. However, the physiology of the human airways is spherical with  
123 symmetric branching, and these features are not present in other species [24].  
124 Moreover, breathing pattern and obligate nose breathing in rodents are also distinct  
125 from humans [12, 25, 26]. Despite those differences, Schlesinger [27] demonstrated a  
126 similar relationship between aerosol size and lung deposition in humans and animals  
127 such as are dogs, rats, guinea pigs, hamsters and mice. However, alveolar distal  
128 impaction reached a peak between 2 and 4  $\mu\text{m}$  in humans but experimental animals  
129 have a peak nearer 1  $\mu\text{m}$ . Some researchers have used mathematic models to study  
130 the aerosol distribution in the airways as an alternative to *in vivo* models [28] but these  
131 methods are highly complex and may not reflect all the conditions that occur *in vivo*.  
132 Imaging techniques, have been used to give a more accurate picture of drug  
133 deposition e.g. radiolabelled inhaled drugs detected by scintigraphic studies [29],  
134 positron emission tomography imaging [30], magnetic resonance imaging [31] or  
135 fluorescent imaging [32]. It is now possible to use a combination of imaging methods  
136 to improve the signal and *in vivo* detection of a system. For example using quantum  
137 dots, which emit a strong fluorescent signal that is not photobleached, coupled with  
138 MRI provides better visualisation than MRI alone [33]. In our studies we have used  
139 luciferin loaded non-ionic surfactant vesicles to show that the drug delivery system

140 (DDS) significantly improves *in vivo* targeting of luciferin to luciferase-expressing cells  
141 within the body.

142



143 **Figure 2** Delivery of luciferin solution (A) compared to luciferin loaded nanocarriers (B;  
144 non-ionic surfactant vesicles, NIVs) to luciferase-expressing cells. Mice, infected  
145 intravenously with  $2 \times 10^7$  luciferase-expressing *Leishmania donovani* promastigotes,  
146 were imaged with luciferin solution (5 mg/ml luciferin in PBS pH 7.4) or luciferin NIVs  
147 (30 mM lipid, 5 mg/ml luciferin in PBS pH 7.4). Bioluminescence was observed using  
148 IVIS imaging system (PerkinElmer, London UK) and represented as photons emitted  
149 per second (C). Treatment with luciferin-NIV delivered significantly more luciferin to  
150 the luciferase-expressing parasites at this time point ( $p \leq 0.001$ ).  
151

## 152 Drug delivery systems

153 Incorporation of drugs into a DDS can improve their therapeutic efficacy by directing  
154 a drug to the correct site for uptake. The lungs are rich in macrophages and 3% of the  
155 cells in the alveolar region are alveolar macrophages and recent studies indicate that  
156 lung macrophages self-renew *in situ* and can repopulate locally after tissue damage  
157 [35]. Macrophages clear particles from the circulation and using a nanoparticulate  
158 DDS will favour macrophage uptake in macrophage-rich tissues and away from urinary  
159 excretion [36, 37]. DDS can be produced in different forms to suit a particular clinical  
160 condition being treated and/or the route of administration e.g. capsules, vesicular  
161 formulations or nanoparticles (NP) and from different constituents e.g. chemically  
162 synthesized or natural products. This review will only consider two types of DDS;  
163 namely non-ionic surfactant vesicles (NIV), and nanoparticles prepared from natural



164 polymers, for pulmonary delivery. There are excellent reviews on using types of DDS  
165 for pulmonary delivery that may be of interest [37, 38, 39].

166

### 167 **Non-ionic surfactant vesicles as a DDS**

168 The properties of NIV depend on their constituents, the relative molar ratio of the  
169 constituents and the method used to prepare the NIV. The inclusion of cholesterol  
170 into NIV helps stabilise the vesicular membrane and modifying the concentration of  
171 cholesterol present in the formulation influences drug loss across the vesicular bilayer.  
172 Inclusion of an amphiphile such as dicetyl phosphate, gives the vesicles a net negative  
173 surface charge, which helps to keep the vesicle dispersed within a suspension and  
174 prevents them clumping [40]. NIV have been used for delivery of a variety of drugs  
175 and hydrophilic drugs are entrapped within the aqueous space formed by the vesicle  
176 bilayers whereas hydrophobic drugs can be incorporated into the lipid bilayers. NIV  
177 can be formed from a single or multiple bilayers depending on the production method.  
178 And the size of the vesicles formed can be reduced using different methods post-  
179 production e.g. sonication, extrusion under high pressure or homogenisation. In our  
180 studies we have used rodent model of visceral leishmaniasis (VL), where animals  
181 infected with the protozoan parasite *Leishmania donovani*, allowed us to study drug  
182 delivery to the spleen, liver and bone marrow in the same animal [34]. In addition, this  
183 model allowed us to investigate local delivery to macrophages as the parasite lives  
184 with macrophages within these sites. We used reduction in parasite burdens as well  
185 as determining antimony levels within tissues as a measure of drug delivery. This was  
186 particularly useful as SSG is a highly water soluble drug and has a short half life. VL is  
187 an important neglected tropical disease, which causes 40,000 deaths/year in the  
188 Indian subcontinent, would benefit from the production of more effective drug  
189 formulations, as there are a limited number of drugs available for treatment [41]. At  
190 present there is only one oral drug licenced for treatment of VL i.e. miltefosine, and  
191 resistance to miltefosine can easily be induced in the laboratory by culturing the  
192 parasite in medium containing increasing amount of miltefosine. Therefore, there is  
193 growing concern that the clinical utility of miltefosine may follow the same path as  
194 SSG especially as incidences of increased resistance to this drug have already been  
195 reported in India [42] and Nepal [43].

196

197 In our initial studies we showed that the NIV could be used to entrap the anti-  
198 leishmanial drug, sodium stibogluconate (SSG), and that the amount of drug  
199 entrapped within vesicles significantly affected their *in vivo* efficacy in different sites.  
200 Thus treatment with SSG-NIV at a dose of 44.4 mg Sb<sup>v</sup>/kg resulted in a significant  
201 reduction in spleen, liver and bone marrow parasite burdens, but only if multiple  
202 doses (i.e. 5 doses) were used [44]. Similar treatment with SSG solution could only  
203 suppress liver parasites burdens in infected mice. Determination of antimony levels  
204 showed that treatment with SSG-NIV resulted in significantly lower blood levels than  
205 similar treatment with free SSG solution and significantly higher amounts of antimony  
206 were detected in the liver at 6 days post-dosing [36]. Increasing the SSG concentration  
207 to prepare SSG-NIV increased the efficacy of the formulation. Thus, single dose  
208 treatment with SSG-NIV, prepared using SSG solution at 33 mg Sb<sup>v</sup>/ml, significantly  
209 suppressed parasite burdens (> 98% compared to controls) in all three sites when  
210 animals were treated with a dose of 296 mg Sb<sup>v</sup>/kg. In contrast similar treatment with  
211 SSG solution only affected hepatic parasite burdens. This SSG-NIV formulation did not  
212 require sonication to reduce vesicle size. It was as effective as AmBisome, a liposomal  
213 formulation of amphotericin [45], and was highly active against clinical strains of  
214 antimony susceptible and antimony resistant *L. donovani* in murine studies [46].  
215 Studies in the dog were carried out to compare the pharmacokinetic and toxicity  
216 profile of SSG solution, SSG-NIV, SSG-dextran solution, and a SSG-NIV-dextran  
217 formulation. The SSG-NIV-dextran formulation was produced using an additional  
218 ultrafiltration step to remove unentrapped SSG, and the dextran was used to balance  
219 the osmotic pressure across the vesicle bilayer, which could result in loss of entrapped  
220 drug. The mean vesicle size was lower for the SSG-NIV-dextran solution and the  
221 entrapment efficiency was seven times higher (mean size: SSG-NIV, 526 nm, SSG-NIV-  
222 dextran 253 nm; entrapment efficiency, SSG-NIV, 6%, SSG-NIV-dextran 43%).  
223 Treatment of dogs with a single intravenous dose of the four SSG formulations (10 mg  
224 Sb<sup>v</sup>/kg) showed that the SSG-NIV-dextran formulation gave a significantly highest  
225 distribution half-life ( $p = 0.01$ ), longest elimination half-live ( $t_{1/2\beta}$ ) and a significantly  
226 higher residence time ( $p = 0.02$ ). There were signs of acute toxicity in dogs treated  
227 with this formulation but not the SSG-NIV formulation, but these were short lived and

228 are probably related to the proportionally higher antimony dose directed to the liver  
229 but the formulation. These could be avoided by simply reducing the drug dose. The  
230 toxic side effects were those expected for antimony and are unlikely to be related to  
231 the DDS as they were absent in dogs treated with the SSG-NIV formulation. Studies  
232 using the same formulations in mice showed that the SSG-NIV-dextran formulation  
233 was more effective than SSG or SSG-NIV even though it was given at a seventh of the  
234 drug dose (33 versus 222 mg Sb<sup>v</sup>/kg, [47]). However further development of the SSG-  
235 NIV formulation was stopped when antimony resistance developed within endemic  
236 parasites became widespread in India, as this may have affected the clinical utility of  
237 this formulation. However, this did not stop development of this DDS as we had  
238 already demonstrated that NIV could be used to increase the *in vivo* efficacy of other  
239 drugs with different physiochemical characteristics [48, 49]. Over the years we have  
240 changed the method used to prepare NIV from a solvent based method to a simple  
241 'melt-method' where the vesicular constituents (surfactant, cholesterol, and dicetyl  
242 phosphate) were melted at 130°C and then hydrated with drug solution at a  
243 temperature of 70°C. We have used homogenisation at different speeds, and for  
244 different periods of time, to reduce vesicle size and we have produced vesicle  
245 suspensions with different means sizes (100-2000 nm range). We have identified a  
246 production method that is suitable for large-scale manufacture, and we have  
247 produced litre batches of NIV drug suspensions.

248

249 The studies on formulating NIV drug formulations for the intravenous route have  
250 helped us develop NIV formulations for administration by the pulmonary route. Using  
251 an amphotericin-NIV formulation (AMB-NIV) as our exemplar we have shown that  
252 treatment of rats infected with *Aspergillus*, an important human pathogen, resulted  
253 in a significant reduction in fungal lung burdens ( $p < 0.01$ ). One dose of AMB-NIV was  
254 as effective as 5 oral doses of the antifungal drug posaconazole [34]. Treatment with  
255 inhaled AMB-NIV resulted in significant higher levels of AMB in the lungs ( $p < 0.05$ )  
256 that similar treatment with AMB solution and significantly lower plasma levels ( $p <$   
257  $0.05$ ). This formulation was also active against *L. donovani* in a murine model when  
258 given by inhalation. Thus treatment with five doses of AMB-NIV resulted in a  
259 significant reduction in liver parasite burdens ( $p < 0.05$ ) but failed to affect splenic or

260 bone marrow burdens compared to controls, the inability to affect parasites in deeper  
261 tissues probably reflects poor drug delivery to these sites. Similar studies using mice  
262 infected in the footpad with luciferase-expressing *L. major*, a species that causes  
263 cutaneous leishmaniasis, showed that NIV did not enhance delivery of luciferin to  
264 parasites at this site based on bioluminescence emitted from the footpad after  
265 treatment. Therefore, it was not surprising that treatment with inhaled AMB-NIV  
266 failed to reduce parasite burdens at this site compared to control values. One of the  
267 problems associated with using the murine model is the practical difficulty  
268 encountered in treating mice by inhalation. In our studies we have exposed mice to  
269 drug formulation by placing them in a Volumetric Spacer, and introducing aerosolised  
270 drug formulations produced using a Buxco® nebulisation system into the Spacer.  
271 Simple calculation of the drug dose administered using the breathing rate of mice  
272 indicates that only a fraction of a dose given is likely to be inhaled by mice. Thus  
273 calculation of the best-case scenario indicated that mice would inhale 17% of the drug  
274 dose given. It is likely to be much lower, mice given luciferin-NIV by inhalation emitted  
275 < 4% of the bioluminescence emitted by mice given the same dose of luciferin-NIV by  
276 the intravenous route [34]. Despite this limitation this model can be used for initial  
277 screening of inhaled formulation, but ideally a larger rodent model should be used in  
278 studies. Other researchers have also determined the feasibility of NIV prepared from  
279 a different surfactant for pulmonary delivery of beclomethasone dipropionate (BDP).  
280 The amount of drug entrapped within BDP-NIV increased as the drug concentration  
281 used to prepare NIV was increased, which is consistent with our findings. The BDP-  
282 NIV had a MMAD of 2  $\mu\text{m}$  indicating that the NV would deposit within the lower  
283 airways of the lungs. In addition, drug permeation studies indicated that the presence  
284 of the non-ionic surfactant increased the ability of the drug to pass through mucin,  
285 using *an in vitro* system [50]. Niosomes (or NIV) containing 5-fluorouracil which were  
286 prepared using different sorbitan monoesters had a mean size of 3.9-8.1  $\mu\text{m}$ , making  
287 some of them too large for inhalation and the smaller ones would be difficult to  
288 aerosolise in a droplet size of < 5  $\mu\text{m}$  required for delivery into the lower airways.  
289 However, another option would be to produce lyophilised formulations that could be  
290 administered as a dry powder using a suitable inhaler. On reaching their deposition

291 site within the lungs the NIV constituents would be hydrated and vesicles, which  
292 would be taken up by the macrophages present [39].

293

#### 294 **Nanoparticles produced from natural polymers as a DDS**

295 A different type of DDS to NIV are nanoparticles, which can give have high drug loading  
296 and are also readily taken up by alveolar macrophages [39]. NP can be produced from  
297 biocompatible polymers from natural proteins or sugars. These types of formulations  
298 are often produced as a lyophilised product and administered using a dry powder  
299 inhaler. This usually requires inclusion of a carrier into the formulation such as lactose,  
300 which prevents the NP clumping together. However, by selecting an appropriate  
301 inhaler e.g. Turbuhaler® it is possible to remove the requirement for a carrier in the  
302 NP formulation [51].

303

304 Three natural proteins can be used to produce NP: collagen, albumin or gluten.  
305 Production of collagen NPs usually requires the use of solvents and a multi-step  
306 method, which would increase manufacture costs. Electrospray methods can be used  
307 but these need to be adapted to ensure that particles rather than fibres are produced  
308 [52]. Collagen NP with a size of  $< 1 \mu\text{m}$  were produced when a salt solution as well as  
309 acetic acid at a concentration of  $< 90\%$  v/v was used. Inclusion of the salt allowed  
310 formation of dried NP particle after spraying and increased the conductivity of the  
311 particles produced. Scanning electron studies showed that changing the salt solution  
312 (i.e sodium chloride vs. calcium chloride), the relative concentration of salt and/or  
313 acetic acid allowed NP with mean sizes between 228-900 nm to be formed. Loading  
314 collagen NP with theophylline, a drug used in the treatment of chronic obstructive  
315 pulmonary disease, resulted in the production of larger particles (size range of 2-3  
316  $\mu\text{m}$ ). And factors such as type of nozzle used (single or coaxial), or cross-linking by  
317 exposing the formulation to glutaldehyde, influenced NP size; and the amount of  
318 cross-linking introduced influenced drug release. No *in vivo* studies were completed  
319 in this study but it did show that collagen nanoparticles of a suitable size range for  
320 lung delivery could be produced using a single step method.

321

322 Albumin NP can be produced using ovalbumin, serum albumin or human albumin.  
323 Human albumin is the most appropriate for clinical drug formulations, as it would not  
324 induce an immune response [53]. Choi and co workers [54] prepared NP using human  
325 serum albumin (HSA) conjugated with doxorubicin and octyl aldehyde. The NP were  
326 coated with TRAIL protein (tumour necrosis factor (TNF)-related apoptosis-inducing  
327 ligand) to improve drug targeting to cancer cells and had a particle size of 342 nm. The  
328 formulation was introduced into the lungs of nude BALB/c bearing lung tumours,  
329 caused by implantation of H226 cells. Mice were treated with the NP formulation by  
330 the pulmonary route using a microsyringe aerosoliser. Treatment resulted in a  
331 significant reduction in tumor burden, based on lung weight and more apoptotic  
332 cancer cells were presented in drug treated mice compared to controls. This  
333 formulation was more effective than NP prepared using doxorubicin and octyl  
334 aldehyde. Data on drug entrapment for this formulation were not given but results  
335 from this study indicate that inclusion of a ligand that can bind to cells can improve  
336 drug targeting. Two albumin NP formulations (termed Nab) have already been given  
337 FDA approval for clinical studies i.e. Nab paclitaxel (Nab-paclitaxel) for the treatment  
338 of metastatic breast cancer when used alone [54] or given in combination with  
339 carboplatin. The overall response rate (42% vs. 23%;  $p = 0.022$ ), and tumour size  
340 shrinkage (37% vs. 20%,  $p = 0.006$ ), was higher in patients with visceral dominant  
341 disease treated with Nab-paclitaxel compared to paclitaxel alone. But there was no  
342 increase in the mean survival rate for Nab-paclitaxel treated patients compared to  
343 paclitaxel treatment alone. Nab-paclitaxel was however given a higher drug dose  
344 compared to paclitaxel alone (Nab-paclitaxel, 260 mg/m<sup>2</sup> every 3 weeks, paclitaxel  
345 175 mg/m<sup>2</sup> every three weeks). Drug doses were not matched, as the objective of the  
346 study was to examine the efficacy and safety of Nab-paclitaxel versus paclitaxel in  
347 patients with poor prognostic factors. The two drugs had a similar toxicity profile but  
348 interestingly the NP formulation was more effective in patients  $\geq 65$  years old (overall  
349 response rates Nab-paclitaxel 27 % vs. 19 % for paclitaxel; progression free survival  
350 5.6 vs. 3.5 months), which is important factor as elderly patients are now more  
351 common within populations [56, 57]. A more effective drug formulation for this cohort  
352 of patients would be beneficial.  
353

354 NP can be made from polysaccharides such as chitosan, hyaluronate, cellulose,  
355 carrageenans, alginate or starch. Chitostan is a cationic polysaccharide usually  
356 produced from chitin by deacetylation. Chitin has a  $pK_a$  of 6.2-6.8, and within an acidic  
357 environment (e.g. within tumour cells); chitosan can remain protonated and will swell.  
358 This would favour quick release of drug at the deposition site of drug-loaded NP.  
359 Chitostan NP loaded with the anticancer drug methylglyoxal, were small (50-100 nm),  
360 and had a net positive charge (+24 mV), and released their drug load within 10-12  
361 hours [58]. The small size of these NP may indicate that the NP have the potential to  
362 be exhaled once they are released into the airways from their aerosol droplet.  
363 Topotecan-loaded NP produced from chitosan were much larger, with a size of 642  
364 nm and a positive surface charge of 35 mV. These NP had a drug entrapment efficiency  
365 of 100% when a topotecan: chitosan ratio of 1:20 was used. In contrast a poly(D,L-  
366 lactide-co-glycolide or PGLA) and topotecan-loaded NP composite, where the NP were  
367 coated in PGLA resulted in a formulation with a lower entrapment efficiency (28%).  
368 This is probably due to drug loss when PGLA cross-linked to chitosan. The composite  
369 particles had a mean size of 2.1  $\mu\text{m}$  and the surface charge dropped to -6.99 mV. A net  
370 negative charge may be beneficial as a positive surface charged has been associated  
371 with cytotoxicity for liposomes [59]. Drug release from the composite particles was  
372 much slower so that only 24% of the entrapped drug was released during the first 24  
373 hours, making these NP suitable for sustained drug release at their uptake site.

374

375 Hyaluronate can also be used to improve targeting to cancer cells as it binds to CD44  
376 and CD168, markers upregulated on cancer cells [60]. NP loaded with paclitaxel and  
377 baicalcein, had a hydrophilic shell of hyaluronate and a hydrophobic core that  
378 contained the drugs. The NP had a mean size of 92 nm and a zeta potential of + 3 mV  
379 and the nanoparticulate formulation was more toxic to A549 cells than paclitaxel/  
380 baicalcein solution alone ( $p < 0.05$ ). Studies in a murine tumour model, where  
381 Kummung mice were injected with paclitaxel resistant A549 cells, showed that a single  
382 intravenous treatment dose significantly inhibited tumor growth ( $p < 0.05$ ). In contrast  
383 similar treatment with the individual drugs had no significant effect on tumour size  
384 compared to controls. Only treatment of mice with paclitaxel or baicalcein solution

385 resulted in a noticeable reduction in weight compared to controls, indicating that the  
386 NP drug formulation had a lower toxicity to mice.

387

388 Ethyl cellulose was used to produce NP by preparing using an oil in water emulsion  
389 solvent technique [60]. The resulting formulation was exposed to spray freeze-drying  
390 or spray drying, to produce nanocomposite microcarriers from the NP, which would  
391 break up to release the NP from the composite in an aqueous environment. The initial  
392 NP had a mean size of 111 nm before spray drying or spray freeze-drying. After  
393 spraying the nanocomposite microcarriers had a mean volume size of 7.2  $\mu\text{m}$  using  
394 spray drying and 12.3  $\mu\text{m}$  for spray freeze-drying. Spray freeze-drying gave particles  
395 that had a much larger surface area (77.6 vs. 2.4  $\text{m}^2/\text{g}$ ) but the MMAD (2.4  $\mu\text{m}$  vs. 3.1  
396  $\mu\text{m}$ ) and GSD (3.1 vs. 2.9) were very similar for the two spraying methods.  
397 Reconstitution of the nanocomposite microcarriers showed that spray freeze-drying  
398 gave a better formulation as it resulted in release of NP with a more uniform size [61].  
399 The results indicate that this method could produce a NP based formulation that was  
400 suitable for pulmonary delivery, that could be administered as an inhalable dry-  
401 powder. Ethyl cellulose or a mixture of ethyl and methyl cellulose were used to  
402 prepare NP that contained an extract from *G. mangostana* Linn, a tropical fruit from  
403 Southeast Asia [61]. The NP had a similar mean size of 253 and 250 nm respectively  
404 and a similar drug entrapment efficiencies (86 vs. 88%). NP prepared from ethyl  
405 cellulose had a more negative  $\zeta$ -potential (-31 vs. -12 mV respectively). Both  
406 formulations were cytotoxic to HeLa cells, with NP prepared using ethyl cellulose being  
407 more cytotoxic ( $\text{IC}_{50}$  values 16.7 vs. 7.4  $\mu\text{g}/\text{ml}$ ). The corresponding extract-free NP had  
408 no toxicity against the cells at the doses used.

409

410 NP were formed from alginate using poly(lactic-co-glycolic acid) [PLGA] and chitostan  
411 or poly(vinyl) alcohol [PVA]. Alginate/PLGA/chitostan NP had an entrapment efficiency  
412 of 71% (502H PGLA) or 80% (756 PGLA) whereas NP containing PVA instead of  
413 chitostan had an entrapment efficiency of 79% (502 H PGLA) or 61% (756 PGLA). NP  
414 that did not contain alginate had very poor drug entrapment (<10%), indicating that  
415 inclusion of alginate gave better drug loading. Tobramycin loading of these NP gave  
416 PV NP with a mean size of 300 nm whereas PGLA 756 NP were larger (400-500 nm).



417 Tobramycin loaded NP formed from alginate/PGLA/chitosan had a higher surface  
418 charge (20 to 40 mV) compared to NP formed from alginate/PGLA/PVA (approximately  
419 -5 mV). Both types of NP released tobramycin slowly so that drug was still present in  
420 the medium at day 40 in *in vitro* drug release studies. The two types of NP were loaded  
421 with rhodamine and produced as a dry powder using a spray drying method. This  
422 method produced larger structures that were termed 'nano-embedded  
423 microparticles' (NEM). The two types of NEM formulations had a similar MMAD  
424 (alginate/502 H PGLA/chitosan, 3.7; alginate/502 H PGLA/PVA, 3.7), with  
425 alginate/502 H PGLA/chitosan NEM having a higher FPF value (38 vs. 52%  
426 respectively). Rats were treated by the pulmonary route with the different NEM  
427 formulation using a breath-activated, reusable DPI to determine where they  
428 deposited in the lungs. Rhodamine alginate/PGLA/chitosan NEM deposited  
429 rhodamine in the trachea, bronchia and bronchioles whereas alginate/PGLA/PVA NEM  
430 deposited rhodamine in the alveolar ducts and not the upper airways [62].

431

432 There are a number of studies on using starch to prepare DDS, as it is one of the main  
433 dietary carbohydrates, and is therefore safe to use in humans. Starch was used to  
434 prepare functionalized graphene nanosheets and loaded with hydroxycamptothecine  
435 (HCPT). 12 µg of HCPT could be loaded in to 150 µg of starch-graphene complex. At  
436 the doses used, co-incubation of SW-620 cells had no cytotoxic effect against cells  
437 whereas treatment with HCPT-starch-graphene or HCPT were toxic to cells. The drug  
438 solution was more effective but this could reflect the slow release of the drug from  
439 the graphene composite. Obviously for pulmonary delivery this type of complex would  
440 have to be manufactured into a suitable size and particle size for inhalation, and  
441 careful selection of the type of graphene to avoid toxicity is required [63].

442

#### 443 **Conclusions**

444 Both NIV and NP produced from natural products can be used to deliver a variety of  
445 drugs by different routes including inhalation. In both cases a switch from batch  
446 manufacture to continuous manufacturing processes would facilitate large-scale  
447 production [64] and studies have shown that spray drying, which could be  
448 incorporated into such a method, is feasible for some formulations. Lactose is often

449 used as a carrier to protect drugs against the harsh environmental conditions present  
450 during spray drying, and it often mixed with drug formulations to improve the  
451 flowability of powders administered using dry powder inhalers [65]. Therefore it is  
452 important to consider what type of device is going to be used for a drug formulation  
453 early on in its development to ensure that the appropriate type of formulation for the  
454 intended delivery device is developed. Three-dimension printing is an area that is  
455 actively being explored for production of production of novel drug formulations but  
456 achieving the small size required for production of nanoparticles is challenging, but  
457 not impossible. Nanoimprint lithography has been used to produce shape-specific  
458 solid NP with sizes of 50-400 nm [66]. And Cylindrical nanoparticles with a diameter  
459 of 240 or 125 nm have been produced using poly (acrylic acid), which could be used  
460 for aqueous or organic solvent-based imprint solutions [66]. Adapting 3-D printing  
461 methods to prepare NP from natural proteins or polysaccharides may be challenging,  
462 but alginate is already been used in preparing 3-D printed hydrogels, as it is a viscous  
463 non-toxic material that cross-linked in the presence of some divalent cations [68]. One  
464 major hurdle for translating a laboratory formulation into a clinical product is  
465 successful completion of preclinical toxicity testing. However it is difficult predict  
466 whether a formulation will indeed be safe even if natural instead of synthetic,  
467 surfactants are used in the DDS as the entrapped therapeutic may be cytotoxic.  
468 However using a surfactant that is biocompatible with humans should reduce the  
469 inherent toxicity of the DDS. At present healthcare providers are struggling to treat  
470 the high number of patients that use public health services, whilst meeting the  
471 constraints of their budget. Production of drug formulations or reformulation of  
472 existing drug for a non-invasive administration route could be a beneficial as it could  
473 reduce treatment costs if patients self-mediate rather than rely on in-patient service  
474 for drugs currently given by the parenteral route. Production of an effective drug  
475 formulation that can be given by inhalation may be facilitated by co-development of  
476 a nebuliser/drug formulation combination, to ensure that the formulation is deposited  
477 in the correct area of the respiratory tract for the particular disease indication.  
478 Technology to produce aerosols of drug formulations has changed to try and controls  
479 some of the 'drug-free' factors that can impact on therapeutic outcome, such as  
480 patient profile (adult versus pediatric use), device used, as well as correct use of the

481 inhalation device by the patient [16, 51, 56]. Therefore testing what impact using  
482 different nebulisers/inhalers has on pulmonary delivery should be an important  
483 consideration in the development of any inhaled drug formulation.

## REFERENCES

1. Pulmonary Drug Delivery Systems Market Expected to Reach USD 28.7 Billion Globally in 2019: Transparency Market Research. Available from: ([www.transparencymarketresearch.com/pulmonary-drug-delivery-systems.html](http://www.transparencymarketresearch.com/pulmonary-drug-delivery-systems.html))
2. Colombo P., Traini D., Buttini F., Inhalation Drug Delivery, First, First edition, Chichester, West Sussex, 2012.
3. Groneberg D.A., Witt C., Wagner U., Chung K.F., Fischer A., Fundamentals of pulmonary drug delivery, *Respir. Med.* 2003; 97: 382-387.
4. Lucangelo U., Pelosi P., Walter A.Z., Aliverti A. Respiratory System and Artificial Ventilation, First edition, New York, 2008.
5. Clarke S.W. Inhaler therapy. *Q. J. Med.* 1988; 67: 355-68.
6. Byron R. Prediction of drug residence times in regions of the human respiratory tract following aerosol inhalation, *J. Pharm. Sci.* 1986; 7: 433-438.
7. Asking L., Olsson B. Calibration at Different Flow Rates of a Multistage Liquid Impinger, *Aerosol Sci. Technol.* 1997; 27: 39-49.
8. Zanen P., Go L.T., Lammers W.J. The optimal particle size for  $\beta$ -adrenergic aerosols in mild asthmatics, *Int. J. Pharm.* 1994; 107: 211-217.
9. Johnson M.A., Newman S.P., Bloom R., Talaei N., Clarke S.W. Delivery of albuterol and ipratropium bromide from two nebulizer systems in chronic stable asthma. Efficacy and pulmonary deposition, *Effic. Pulm. Depos. Chest.* 1989; 96: 6-10.
10. Patton J.S., Byron P.R. Inhaling medicines: delivering drugs to the body through the lungs. *Nat. Rev. Drug Discov.* 2007; 6: 67-74.

11. Dolovich M., Sanchis J., Rossman C., Newhouse M. Aerosol penetrance: a sensitive index of peripheral airways obstruction, *J. Appl. Physiol.* 1976; 40: 468-471.
12. Nahar K., Gupta N., Gauvin R., Absar S., Patel B., V. Gupta V., Ali Khademhosseini A., Ahsanaet F. *In vitro*, *in vivo* and *ex vivo* models for studying particle deposition and drug absorption of inhaled pharmaceuticals. *Eur. J. Pharm. Sci.* 2013; 49: 805–818.
13. Hillery A.M., Lloyd A.W., Swarbrick J. *Drug delivery and targeting for pharmacists and pharmaceutical scientists*, First edition, 2001.
14. Hu T., Wang J., Shen Z., Chen J. Engineering of drug nanoparticles by HGCP for pharmaceutical applications. *Particology.* 2008; 6: 239-251.
15. Dolovich M.B., Dhand R. Aerosol drug delivery: developments in device design and clinical use. *Lancet.* 2011; 377: 1032-1045.
16. Lavorini F., Fontana G.A., Usmani O.S. New inhaler devices - The good, the bad and the ugly. *Respiration.* 2014; 88: 3-15.
17. European Pharmacopeia, 2.9.18 Preparations for inhalation: aerodynamic assessment of fine particles, *Prep. Inhal.* 2005; 5.1: 2799-2811.
18. Aerosols, nasal sprays, metered-dose inhalers, and dry powder inhalers. Available at ([http://www.pharmacopeia.cn/v29240/usp29nf24s0\\_c601\\_viewall.html](http://www.pharmacopeia.cn/v29240/usp29nf24s0_c601_viewall.html))
19. Boer A.H., Gjaltema D., Hagedoorn P., Frijlink H.W. Characterization of inhalation aerosols: a critical evaluation of cascade impactor analysis and laser diffraction technique. *Int. J. Pharm.* 2002; 249: 219-231.

20. Triballier K., Dumouchel C., Cousin J. A technical study on the Spraytec performances: influence of multiple light scattering and multi-modal drop-size distribution measurements. *Exp. Fluids*. 2003; 35: 347-356.
21. Pilcer G., Vanderbist F., Amighi K. Correlations between cascade impactor analysis and laser diffraction techniques for the determination of the particle size of aerosolised powder formulations. *Int. J. Pharm.* 2008; 358: 75-81.
22. Cheng Y., Irshand H., Kuehl P., Holmes T., Sherwood R., Hobbs C. Lung deposition of droplet aerosols in monkeys. *Inhal. Toxicol.* 2008; 11: 1029-1036.
23. Oller A.R., Oberdörster G. Incorporation of particle size differences between animal studies and human workplace aerosols for deriving exposure limit values, *Regul. Toxicol. Pharmacol.* 2010; 57: 181-194.
24. Miller F.J., Mercer R.R., Crapo J.D. Lower Respiratory Tract Structure of Laboratory Animals and Humans: Dosimetry Implications, *Aerosol Sci. Technol.* 1993; 18: 257-271.
25. Sakagami M. *In vivo*, *in vitro* and *ex vivo* models to assess pulmonary absorption and disposition of inhaled therapeutics for systemic delivery. *Adv. Drug Deliv. Rev.* 2006; 58:1030-1060.
26. Cryan S.A. , Sivadas N., Garcia-Contreras L. *In vivo* animal models for drug delivery across the lung mucosal barrier. *Adv. Drug Deliv. Rev.* 2007; 59: 1133-1151.
27. R.B. Schlesinger, Comparative deposition of inhaled aerosols in experimental animals and humans: a review., *J. Toxicol. Environ. Health.* 1985; 15: 197-214.
28. Patel B., Gauvin R., Absar S., Gupta V., Gupta N., K. Nahar K., Khademhosseini A., Ahsan F. Computational and bioengineered lungs as alternatives to whole animal, isolated organ, and cell-based lung models. *Computational and bioengineered lungs as alternatives to whole animal, isolated organ, and cell-based lung models*

Computational and bioengineered lungs as alternatives to whole animal, isolated organ, and cell-based lung models, *Am. J. Physiol. Lung Cell. Mol. Physiol.* 2012; 303: 733-747.

29. Newman S., Scintigraphic assessment of therapeutic aerosols, *Crit. Rev. Ther. Drug Carrier Syst.* 1993; 10: 65-109.

30. Pérez-Campaña C., Gómez-Vallejo V., Puigivila M., Martin A., Calvo-Fernández T., Moya S.E., Larsen S.T., Gispert J.D., Llop J.C. Assessing lung inflammation after nanoparticle inhalation using 2-deoxy-2-[18F]Fluoro-d-glucose positron emission tomography imaging. *Mol. Imaging Biol.* 2014; 16: 264-273.

31. Thompson R., Finlay W. Using MRI to measure aerosol deposition, *J. Aerosol Med. Pulm. Drug Deliv.* 2012; 25: 55-62.

32. Yi D., Naqwi A., Panoskaltzis-Mortari A., Wiedmann T.S. Distribution of aerosols in mouse lobes by fluorescent imaging. *Int. J. Pharm.* 2012; 426: 108-115.

33. Walia S., Acharya A. Silica micro/nanospheres for theranostics: from bimodal MRI and fluorescent imaging probes to cancer therapy., *Beilstein J. Nanotechnol.* 2015; 6: 546-558.

34. Alsaadi M., Italia J.L., Mullen A.B., Kumar R.M.N., Candlish A.A., Williams R.A., Shaw C.D., Al Gawhari F., Coombs G.H., Wiese M., Thomson A.H., Puig-Sellart M., Wallace J., Sharp A., Wheeler L., Warn P., Carter K.C. The efficacy of aerosol treatment with non-ionic surfactant vesicles containing amphotericin B in rodent models of leishmaniasis and pulmonary aspergillosis infection, *J. Control. Release.* 2012; 160: 685-691.

35. Hashimoto D., Chow A., Noizat C., P. Teo P., Beasley M.B., Leboeuf M., Becker C.D., See P., Price J., Lucas D., Greter M., Mortha A., Boyer S.W., Forsberg E.C., Tanaka M., van Rooijen N., García-Sastre A., Stanley E.R., Ginhoux F., Frenette P.S., Merad M.

Tissue-Resident Macrophages Self-Maintain Locally throughout Adult Life with Minimal Contribution from Circulating Monocytes, *Immunity*. 2013; 38: 792-804.

36. Collins M., Carter K., Baillie A., O'Grady J. The Distribution of Free and Non-Ionic Vesicular Sodium Stibogluconate in the Dog. *J. Drug Target*. 1993; 1: 133-142.

37. Kraft J.C., Freeling J.P., Wang Z., Ho R.J.Y. Emerging Research and Clinical Development Trends of Liposome and Lipid Nanoparticle Drug Delivery Systems,=. *J. Pharm. Sci*. 2014; 103: 29-52.

38. Moreno-Sastre M., Pastor M., Salomon C.J., Esquisabel A., Pedraz J.L. Pulmonary drug delivery: a review on nanocarriers for antibacterial chemotherapy. *J Antimicrob Chemother*. 2015; 70: 2945-2955.

39. Pham D.D., Fattal E., Tsapis N. Pulmonary drug delivery systems for tuberculosis treatment. *Int J Pharm*. 2015; 478: 517-529.

40. Uchegbu I. F., Florence A. T. Non-ionic surfactant vesicles (niosomes): Physical and pharmaceutical chemistry. *Advances in Colloid and Interface Science*. 1995; 58: 1-55.

41. Alvar J., Velez I.D., Bern C., Herrero M., Desjeux P., Cano J., Jannin J., den Boer M., WHO Leishmaniasis Control Team. Leishmaniasis worldwide and global estimates of its incidence. *PLoS ONE* 2012; 7: e35671.

42. Sundar S., Singh A., Rai M., Prajapati V.K., Singh A.K., Ostyn B., Boelaert M., Dujardin J.C., Chakravarty J. Efficacy of miltefosine in the treatment of visceral leishmaniasis in India after a decade of use. *Clin Infect Dis*. 2012; 55: 543-50.

43. Rijal S., Ostyn B., Uranw S., Rai K., Bhattarai N.R., Dorlo T.P., Beijnen J.H., Vanaerschot M., Decuypere S., Dhakal S.S., Das M.L., Karki P., Singh R., Boelaert M., Dujardin J.C. Increasing failure of miltefosine in the treatment of kala-azar in Nepal



and the potential role of parasite drug resistance, reinfection, or noncompliance. Clin. Infect. Dis. 2013; 56:1530-1538.

44. Carter K.C., Dolan T.F., Alexander J., Baillie A.J., McColgan C. Characteristics and the ability to clear parasites from the liver, spleen and bone marrow in *Leishmania donovani* infected BALB/c mice. J Pharm Pharmacol. 1989; 2:87-91.

45. Mullen A.B., Carter K.C., Baillie A.J. Comparison of the efficacies of various formulations of amphotericin B against murine visceral leishmaniasis. Antimicrob Agents Chemother. 1997; 41:2089-2092.

46. Carter K.C., Mullen A.B., Sundar S., Kenney R.T. Efficacies of vesicular and free sodium stibogluconate formulations against clinical isolates of *Leishmania donovani*. Antimicrob Agents Chemother. 2001; 45: 3555-3559.

47. Nieto J., Alvar J., Mullen A.B., Carter K.C., Rodríguez C., San Andrés M.I., San Andrés M.D., Baillie A.J., González F. Pharmacokinetics, toxicities, and efficacies of sodium stibogluconate formulations after intravenous administration in animals. Antimicrob Agents Chemother. 2003; 47:2781-7.

48. Mullen A.B., Carter K.C., Baillie A.J. Comparison of the efficacies of various formulations of amphotericin B against murine visceral leishmaniasis. Antimicrob Agents Chemother. 1997; 41:2089-92.

49. Williams D, Mullen A.B., Baillie A.J., Carter K.C. Comparison of the efficacy of free and non-ionic-surfactant vesicular formulations of paromomycin in a murine model of visceral leishmaniasis. J Pharm Pharmacol. 1998; 50:1351-6.

50. Terzano C., Allegra L., Alhaique F., Marianecchi C., Carafa M. Non-phospholipid vesicles for pulmonary glucocorticoid delivery. Eur J Pharm Biopharm. 2005; 59:57-62.

51. Stein S.W., Sheth P., Hodson P.D., Myrdal P.B. Advances in Metered Dose Inhaler Technology: Hardware Development, AAPS PharmSciTech. 2014; 15: 326-338.
52. Nagarajan U., Kawakami K., Zhang S., Chandrasekaran B., Unni Nair B. Fabrication of Solid Collagen Nanoparticles Using Electrospray Deposition. Chem. Pharm. Bull. 2014; 62: 422-428.
53. Elzoghby A.O., Samy W.M., Elgindy N.A. Albumin-based nanoparticles as potential controlled release drug delivery systems., J. Control. Release. 2012: 157:168-182.
54. Choi S.H., Byeon H.J., Choi J.S., Thao L., Kim I., Lee E.S., Shin B.S., Lee K.C., Youn Y.S. Inhalable self-assembled albumin nanoparticles for treating drug-resistant lung cancer. J Control Release. 2015; 10: 199-207
55. O'Shaughnessy J., Gradishar W.J., Bhar P., Iglesias J. Nab-paclitaxel for first-line treatment of patients with metastatic breast cancer and poor prognostic factors: a retrospective analysis. Breast Cancer Res Treat. 2013; 138:829-837
56. Grootjans-van Kampen I., Engelfriet P.M. van Baal P.H. Disease Prevention: Saving Lives or Reducing Health Care Costs? PLoS One. 2014; 9: e104469.
57. Minuti G., D'Incecco A., F. Cappuzzo F. Current and Emerging Options in the Management of EGFR Mutation-Positive Non-Small-Cell Lung Cancer: Considerations in the Elderly, Drugs Aging. 2015: 7: 1-10.
58. Pal A., Talukdar D., Roy A., Ray S., Mallick A., Mandal C., Ray M. Nanofabrication of methylglyoxal with chitosan biopolymer: a potential tool for enhancement of its anticancer effect. Int. J. Nanomedicine. 2015: 10: 3499-3518.
59. Immordino M.L., Dosio F., Cattel L. Stealth liposomes: review of the basic science, rationale, and clinical applications, existing and potential. Int J Nanomedicine. 2006; 1:297-315.

60. Mizrahy S., Raz S.R., Hasgaard M., Liu H., Soffer-Tsur N., Cohen K., Dvash R., Landsman-Milo D., Bremer M.G., Moghimi S.M., Peer D. Hyaluronan-coated nanoparticles: The influence of the molecular weight on CD44-hyaluronan interactions and on the immune response. *J. Control. Release.* 2011; 156: 231-238.
61. Pan-In P., Wanichwecharungruang S., Hanes J., Kim A.J. Cellular trafficking and anticancer activity of *Garcinia mangostana* extract-encapsulated polymeric nanoparticles. *Int J Nanomedicine.* 2014; 9: 3677-3686.
62. Ungaro F., d'Emmanuele di Villa Bianca R., Giovino C., Miro A., Sorrentino R., Quaglia F., La Rotonda M.I. Insulin-loaded PLGA/cyclodextrin large porous particles with improved aerosolization properties: *in vivo* deposition and hypoglycaemic activity after delivery to rat lungs. *J. Control. Release.* 2009; 135: 25-34.
63. Sanchez V.C., Jachak A., Hurt R.H., Kane A.B. Biological interactions of graphene-family nanomaterials: an interdisciplinary review. *Chem. Res. Toxicol.* 2012; 25: 15-34.
64. Hernandez R. Continuous Manufacturing: A Changing Processing Paradigm, *BioPharm Int.* 2015; 28: 20 -27.
66. Rahimpour Y., Hamishehkar H. Lactose engineering for better performance in dry powder inhalers. *Adv Pharm Bull.* 2012;2:183-187. 65. Glangchai L.C., Caldorera-Moore M., Shi L., Roy K. Nanoimprint lithography based fabrication of shape-specific, enzymatically-triggered smart nanoparticles, *J. Control. Release.* 2008; 125: 263-272.
67. Agarwal R., Singh V., Journey P., Shi L., Sreenivasan S.V., Roy K. Scalable imprinting of shape-specific polymeric nanocarriers using a release layer of switchable water solubility. *ACS Nano.* 2012; 6: 2524-2531.

68. Poldervaart M.T., Wang H., van der Stok J., Weinans H., Leeuwenburgh S.C., Öner F.C., Dhert W.J., Alblas J. Sustained release of BMP-2 in bioprinted alginate for osteogenicity in mice and rats. *PLoS One*. 2013; 8: e72610.

69. Rubin B.K. Pediatric aerosol therapy: new devices and new drugs. *Respir. Care*. 2011; 56: 1411-1421.